DOI: https://doi.org/10.62985/j.huit_ojs.vol26.no2E.398

GENERALIZED FAULT TOLERANT CONTROL METHOD FOR DUAL THREE-PHASE PMSM USING PERMUTATION REDUCED-ORDER MATRIX

Pham Le Tam[1,*], Nguyen Ngac Ky[2,*], Phan Quoc Dung[3,†,‡]

[*]*Univ. Lille, Arts et Métiers Institut of Technology,*

Centrale Lille, Yncréa Hauts-de-France ULR 2697-L2EP, F-59000 Lille, France

[†]*Falcuty of Electrical and Electronics Engineering,*

Ho Chi Minh City University of Technology, Ho Chi Minh City, Vietnam

[‡]*Vietnam National University Ho Chi Minh City (VNU-HCM), Ho Chi Minh City, Vietnam*

Email: [1]*le_tam.pham@ensam.eu,* [2]*ngacky.nguyen@ensam.eu*, [3]*pqdung@hcmut.edu.vn*

Received: 15 January 2026; Revised: 8 March 2026; Accepted: 18 April 2026

ABSTRACT

This paper proposes a generalized fault-tolerant control strategy for dual three-phase permanent-magnet synchronous machines (DT-PMSMs) based on a Permutation Reduced-Order Matrix Fault-Tolerant Control (PROM-FTC) method. The approach analytically characterizes the current relationships under any single open-phase fault by introducing a permutation matrix. This enables the automatic and accurate computation of the reference currents without relying on lookup tables or if–else structures. Regarding objective function, the stator copper loss minimization strategy is used to find the optimal currents. The proposed method is validated in MATLAB/Simulink through a sequence of six individual open-phase faults. Simulation results demonstrate that PROM-FTC maintains constant electromagnetic torque during all faulty cases. Additionally, an analysis of stationary current trajectories is conducted to characterize the behavior of each fault scenario, resulting in an effective approach for fault detection and localization. These results confirm the efficacy and generality of the proposed PROM-FTC strategy for DT-PMSMs.

Keywords: Fault-tolerant control, PMSM, dual three-phase, loss minimization, electrical drive.

1. INTRODUCTION

DT-PMSMs have emerged as a leading technology in modern industry, particularly in sectors demanding high power density and reliability. Their architecture, which features two independent three-phase windings, offers significant advantages over conventional three-phase machines, including enhanced power/torque sharing [1], smoother torque output, and higher fault tolerance [2]. These features make DT-PMSM especially attractive for aerospace and other safety-critical applications, where uninterrupted operation is essential [3]. DT-PMSMs can satisfy these sectors as they provide the ability to continue functioning even of one phase fails, thus reducing the risk of catastrophic failure [4].

However, the increased complexity of these machines introduces new challenges, particularly in fault-tolerant control (FTC). Single open-phase faults, where a phase becomes disconnected, are among the most common and disruptive issues, leading to unbalanced currents, increased losses, and torque ripple [5]. In order to achieve effective control of DT-PMSM drive system under open-phase faults, some scholars proposed FTC strategy based on the reduced-dimension model [6], [7]. However, with this type of control strategy, different

decoupling transformations and modulation strategies need to be constructed according to different fault states. Therefore, the FTC structure is complicated since it needs 6 different matrices for 6 phase fault cases. Another class is based on full-dimensional models, which eliminates the need to reconfigure the transformation matrix or the control scheme during faults [8]-[10]. However, because open-phase faults impose constraints on the stator currents, electrical coupling inevitably appears between the different subspaces. Moreover, only one specific fault scenario is evaluated while the reference currents must be recalculated for each different faulty case. In simulation and real-time embedded system, this requires additional mechanisms, such as lookup tables or extensive *if–else* structures.

This article proposes a general FTC method called PROM-FTC. In this approach, the machine reference currents are automatically identified according to the faulty phase location by using a permutation matrix together with a reduced-order transformation model. This eliminates the need for lookup tables or if–else structures, significantly reducing the computational burden and memory footprint for real-time digital implementation compared to conventional condition-based methods.

It should be noted that the proposed PROM-FTC focuses exclusively on the generalized generation of optimal fault-tolerant current references based on the machine's spatial configuration. In this study, the validation was conducted under the assumption of constant motor parameters (stator resistance and inductance), utilizing standard PI controllers for current tracking. If the machine operates under high magnetic saturation where these electrical parameters vary significantly, the tracking performance of the standard PI controllers may degrade. To ensure precise reference tracking and maintain overall drive performance under such nonlinear conditions, the PI controllers should be replaced with more advanced and robust control strategies, such as Model Predictive Control (MPC).

The proposed method is evaluated in MATLAB/Simulink under constant torque operation. In addition, the trajectories of the stationary currents are analyzed for all fault conditions, which are rarely addressed in other studies due to the absence of a general FTC.

2. MATHEMATICAL MODEL OF DUAL THREE-PHASE PMSM

Fig. represents the configuration of a DT-PMSM drive with two isolated neutral points (2N). In this work, the electrical phase shift between two winding sets is $\gamma = \pi/6$. Additionally, the VSD is used to represent the DT machine into two orthogonal subspaces, which are (α, β) and (X, Y). Moreover, the rotor is of the non-salient type, and only the fundamental component of the back-EMF is considered.

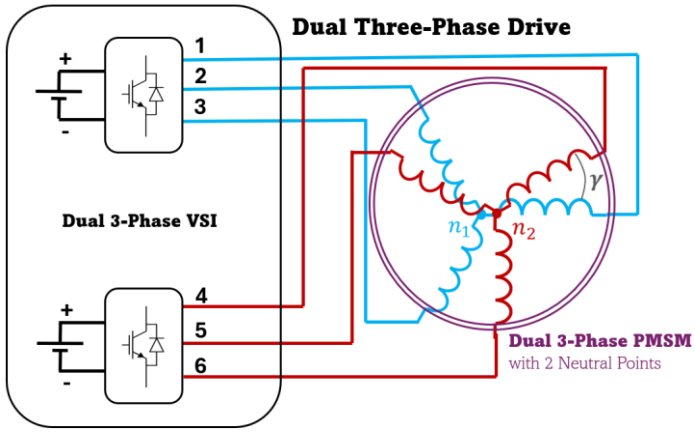

Fig. 1. Dual Three-Phase Drive Configuration [6]

2.1. Vector Space Decomposition

The VSD is to transform the six stator variables into orthogonal subspaces [6]. The Clarke transformation matrix T_{46} which maps the six phase quantities into the $\alpha\beta, XY$ subspaces is defined as (in neglecting the zero-sequence subspaces thanks to the two isolated neutral points):

$$T_{46} = \frac{1}{\sqrt{3}} \begin{bmatrix} 1 & -\frac{1}{2} & -\frac{1}{2} & \frac{\sqrt{3}}{2} & -\frac{\sqrt{3}}{2} & 0 \\ 0 & \frac{\sqrt{3}}{2} & -\frac{\sqrt{3}}{2} & \frac{1}{2} & \frac{1}{2} & -1 \\ 1 & -\frac{1}{2} & -\frac{1}{2} & -\frac{\sqrt{3}}{2} & \frac{\sqrt{3}}{2} & 0 \\ 0 & \frac{\sqrt{3}}{2} & -\frac{\sqrt{3}}{2} & -\frac{1}{2} & -\frac{1}{2} & 1 \end{bmatrix} \quad (1)$$

Using this matrix, the variables in the stationary reference frame are obtained as:

$$[v_\alpha \quad v_\beta \quad v_X \quad v_Y]^T = \mathrm{T}_{46} \times [v_1 \quad v_2 \quad v_3 \quad v_4 \quad v_5 \quad v_6]^T \quad (2)$$

where v_1 to v_6 are phase-to-neutral voltages as illustrated in Fig., corresponding to $v_{A_1}, v_{B_1}, v_{C_1}, v_{A_2}, v_{B_2}, v_{C_2}$.

The transformation from the stationary frame to the rotating frame is given by:

$$[v_d \quad v_q \quad v_{d_z} \quad v_{q_z}]^T = \begin{bmatrix} P(\theta_e) & 0_{22} \\ 0_{22} & P(\theta_e) \end{bmatrix} [v_\alpha \quad v_\beta \quad v_X \quad v_Y]^T \quad (3)$$

where $P(\theta_e) = \begin{bmatrix} \cos(\theta_e) & \sin(\theta_e) \\ -\sin(\theta_e) & \cos(\theta_e) \end{bmatrix}$, $0_{22} = \begin{bmatrix} 0 & 0 \\ 0 & 0 \end{bmatrix}$

2.2. Dynamic Model

The resulting dynamic equations of the DT-PMSM in the rotating VSD frame are:

$$v_d = R_s i_d + L\frac{di_d}{dt} - \omega_e L_q i_q \quad (4)$$

$$v_q = R_s i_q + L\frac{di_q}{dt} + \omega_e \mathrm{L} i_d + \sqrt{3} p \omega_e \psi_f \quad (5)$$

$$v_{dz} = R_s i_{d_z} + L_z\frac{di_{d_z}}{dt} - \omega_e L_\mathrm{z} i_{qz} \quad (6)$$

$$v_{qz} = R_s i_{q_z} + L_z\frac{di_{q_z}}{dt} + \omega_e L_\mathrm{z} i_{dz} \quad (7)$$

Finally, the electromagnetic torque is expressed as:

$$\Gamma_{em} = \sqrt{3} p \psi_f i_q \quad (8)$$

3. PERMUTATION REDUCED-ORDER MATRIX FAULT TOLERANT CONTROL

The primary objective of FTC is to preserve the constant torque despite the loss of a phase. To achieve this, the fundamental currents (i_α, i_β) must maintain their pre-fault trajectories. However, the fault physically reduces the system's degrees of freedom (DoF). In secondary subspace (i_X, i_Y), one current becomes algebraically constrained by the fault condition, while the remaining is available for optimization. The main challenge is that this algebraic constraint shifts by the fault location (e.g., $i_X = -i_\alpha$ and i_Y is independent if A1 opens; $i_Y = i_\beta$ and i_X is independent if C2 opens).

To address this, the PROM-FTC introduces a permutation scheme to formalize this shift based on the faulty star index $m \in \{1,2\}$. Moreover, a reduced-order matrix T_{44} is presented to simplify the faulty condition. A method to define T_{44} from T_{46} is introduced by using a selection matrix I_{64}^{m}. Furthermore, an optimization scheme is proposed wherein PROM-FTC automatically synthesizes the optimal reference functions for (i_X, i_Y) as a function of (i_α, i_β).

3.1. Generalization

Firstly, it is useful to review the equation of stationary currents, as shown in (9):

$$[i_\alpha \quad i_\beta \quad i_X \quad i_Y]^T = T_{46} \times [i_1 \quad i_2 \quad i_3 \quad i_4 \quad i_5 \quad i_6]^T \tag{9}$$

Denote m as the faulty 3-ph star index, $m \in \{1; 2\}$ which corresponds to 3-ph set $\{123; 456\}$. Define j as the arbitrary faulty phase, so the faulty 3-ph set is (j, k, l) can be either $\{123\}$ or $\{456\}$. The relationships of currents under faulty condition are shown as below:

$$i_j = 0;\ i_k = -i_l \tag{10}$$

From (10), it is stated that all elements of column j^{th} in T_{46} are now useless in (9) as they are multiplied with zero. Moreover, the two currents i_k, i_l can be combined into a single one. Correspondingly, the columns k^{th}, l^{th} in T_{46} are combined into a single column of their subtraction. For instance, if phase 3 (phase C_1) opens, $i_3 = 0$ while $i_1 = -i_2$, and the stationary currents can be found as:

$$\begin{bmatrix} i_\alpha \\ i_\beta \\ i_X \\ i_Y \end{bmatrix} = \begin{bmatrix} 3/2 & \sqrt{3}/2 & -\sqrt{3}/2 & 0 \\ -\sqrt{3}/2 & 1/2 & 1/2 & -1 \\ 3/2 & -\sqrt{3}/2 & \sqrt{3}/2 & 0 \\ -\sqrt{3}/2 & -1/2 & 1/2 & 1 \end{bmatrix} \times \begin{bmatrix} i_1 \\ i_4 \\ i_5 \\ i_6 \end{bmatrix} \tag{11}$$

It is observed that the size of transformation matrix used in (11) is reduced from 4x6 to 4x4, compared to the one in (9). It is called reduced-ordered matrix T_{44}.

To generally represent T_{44} from T_{46}, a selection matrix I_{64}^{jkl} is introduced as:

$$T_{44} = T_{46} \times I_{64}^{jkl} \tag{12}$$

where I_{64}^{jkl} initially is the 6x6 elementary matrix, but its j^{th}column is removed while k^{th} and l^{th} columns are combined into their subtraction. For example, the matrix T_{44} in (11) can be found as:

$$T_{44} = \begin{bmatrix} 1 & -1/2 & -1/2 & \sqrt{3}/2 & -\sqrt{3}/2 & 0 \\ 0 & \sqrt{3}/2 & -\sqrt{3}/2 & 1/2 & 1/2 & -1 \\ 1 & -1/2 & -1/2 & -\sqrt{3}/2 & \sqrt{3}/2 & 0 \\ 0 & \sqrt{3}/2 & -\sqrt{3}/2 & -1/2 & -1/2 & 1 \end{bmatrix} \times \begin{bmatrix} 1 & 0 & 0 & 0 \\ 0 & 0 & 0 & 0 \\ -1 & 0 & 0 & 0 \\ 0 & 1 & 0 & 0 \\ 0 & 0 & 1 & 0 \\ 0 & 0 & 0 & 1 \end{bmatrix} \tag{13}$$

Under one phase opening condition, it is confirmed that there are only three independent currents with isolated-neutral-point configuration and (i_α, i_β) must be maintained as pre-fault values. Therefore, only one current in (i_X, i_Y) now is independent for optimization, and the remaining must change their waveform to compensate the fault.

Taking example of phase 3 (phase C_1) opens as above, the current i_X can be expressed as:

$$i_X = -i_\alpha - \sqrt{3} i_\beta - \sqrt{3} i_Y = K_1 i_\alpha + K_2 i_\beta + K_3 i_Y \tag{14}$$

These parameters $\{K_1; K_2; K_3\}$ in (14) are obtained based on a pseudo-inverse method, which is introduced as below:

$$[K_1, K_2, K_3] = T_{44}(3,:) \times pinv\big(T_{44}([1,2,4],:)\big) \tag{15}$$

However, the problem of general FTC is the dependency shift among (i_X, i_Y), where i_Y is independent for all faulty cases in star 1, while i_X is independent for all faulty cases in star 2. As a result, (15) is changed for each case of faulty star.

To address this issue, a general scheme is proposed by this literature.

Denote currents (i_{Z_1}, i_{Z_2}) can be either (i_X, i_Y) or (i_Y, i_X). There will be a swap between the third row and fourth row in T_{44} if the fault occurs in star 1, otherwise there is no swap. It reflects that i_Y is independent in faulty star 1, while i_X is independent in fault of the 2nd star. A matrix T_m is introduced for this swap by using permutation matrix P_4^m as:

$$T_m = (P_4)^{\mathrm{m}} \times \mathrm{T}_{44} \text{ where } P_4 = \begin{bmatrix} 1 & 0 & 0 & 0 \\ 0 & 1 & 0 & 0 \\ 0 & 0 & 0 & 1 \\ 0 & 0 & 1 & 0 \end{bmatrix} \text{ and } m \in (1,2) \tag{16}$$

The parameters $[K_1, K_2, K_3]$ can be generally expressed as in (17) for any case of faults:

$$[K_1 \quad K_2 \quad K_3] = T_{44}(4,:) \times pinv\big(T_{44}([1:3],:)\big) \tag{17}$$

The current i_{Z_2} now can be expressed as:

$$i_{Z_2} = [K_1 \quad K_2 \quad K_3] \times [i_\alpha \quad i_\beta \quad i_{Z_1}]^T \tag{18}$$

Fig. represents the relationship between i_{Z_2} and three independent currents $\{i_\alpha, i_\beta, i_{Z_1}\}$.

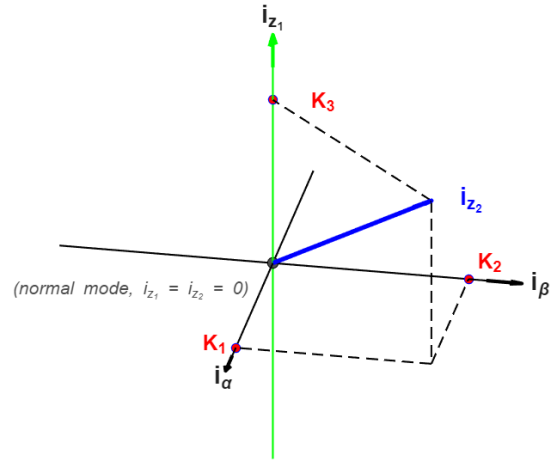

Fig. 2. 3-D plane where i_{z_2} is represented by three independent currents $i_\alpha, i_\beta, i_{Z_1}$

3.2. Optimization Stage

The objective of this stage is to find optimal waveform of currents $\big(i_{d_z}, i_{q_z}\big)$, currents in the 2nd plan in the rotor frame, via (i_X, i_Y), which are the functions of $\big(i_\alpha, i_\beta\big)$. Therefore, i_α and i_β firstly are computed from i_d and i_q as:

$$[i_\alpha \quad i_\beta]^{\mathrm{T}} = P^{-1}(\theta_e) \times [i_d \quad i_q]^{\mathrm{T}} \tag{19}$$

where $i_d = 0; i_q = \Gamma_{em}/\sqrt{3}p\psi_f$.

The copper-loss minimization objective is:

$$f = \min\big(i_{Z_1}^2 + i_{Z_2}^2\big) \tag{20}$$

From (18) and (20), the optimal function becomes:

$$f = i_{Z_1}^2 + \left(K_1 i_\alpha + K_2 i_\beta + K_3 i_{Z_1}\right)^2 \tag{21}$$

Using gradient-descent method to find optimized variable:

$$\frac{\partial f}{\partial i_{Z_1}} = 0 \Longrightarrow 2K_3\left(K_1 i_\alpha + K_2 i_\beta + K_3 i_{Z_1}\right) + 2i_{Z_1} = 0 \tag{22}$$

$$\Longrightarrow i_{Z_1} = \frac{-K_3\left(K_1 i_\alpha + K_2 i_\beta\right)}{1 + K_3^2}, \qquad i_{Z_2} = \frac{K_1 i_\alpha + K_2 i_\beta}{1 + K_3^2} \tag{23}$$

If fault occurs in the first star:

$$[i_X \quad i_Y] = [i_{Z_2} \quad i_{Z_1}] \tag{24}$$

If the fault occurs in the second star:

$$[i_X \quad i_Y] = [i_{Z_1} \quad i_{Z_2}] \tag{25}$$

A permutation matrix P_2 is defined as:

$$[i_X \quad i_Y]^T = P_2^m [i_{Z_1} \quad i_{Z_2}]^T, \qquad P_2 = \begin{bmatrix} 0 & 1 \\ 1 & 0 \end{bmatrix} \tag{26}$$

where $m \in (1,2)$ is faulty star index.

Thus, the general expression for (i_X, i_Y) is:

$$[i_X \quad i_Y]^T = P_2^m \left[\frac{-K_3\left(K_1 i_\alpha + K_2 i_\beta\right)}{1 + K_3^2} \quad \frac{K_1 i_\alpha + K_2 i_\beta}{1 + K_3^2}\right]^T \tag{27}$$

Eventually, the reference values of currents (i_{d_z}, i_{q_z}) can be obtained as:

$$[i_{d_z} \quad i_{q_z}]^T = P(\theta)^{-1} [i_X \quad i_Y]^T \tag{28}$$

Fig. represents the vector control scheme, which add an option of PROM-FTC in determining the reference currents i_{d_z}, i_{q_z}.

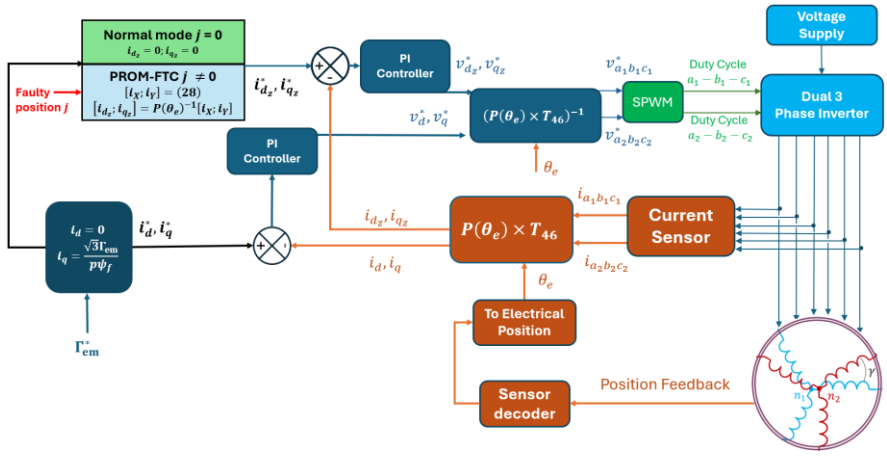

Fig. 3. Vector Control Scheme of DT-PMSM with PROM-FTC

4. SIMULATION RESULTS

To verify the effectiveness of the proposed strategy, a simulation model was established in MATLAB/Simulink. The parameters of the DT drive are provided in Table.

Fig. illustrates the sinusoidal waveforms of back-EMF which are imposed from the machine. Only the fundamental components are considered in this simulation.

To analyze the effect of open-phase fault, the machine was conducted when A1 open from 0.39s, as shown in Fig. Right after phase A_1 open, the torque control is lost when its waveform becomes resonant as shown in Fig. 6. That's due to the resonant waveforms of dynamic frames currents in Fig.

Fig. illustrates the relationship of stationary currents. In the normal mode, (i_α, i_β) trace circular trajectories, while (i_X, i_Y) is a single point at the origin as both components are zero. When A1 opens, (i_α, i_β) distorts from a perfect circle into a *quasi-elliptical path*, reflecting the loss of symmetry in the fundamental flux. Simultaneously, the (i_X, i_Y) currents expand from the origin to a complex *butterfly-shaped trajectory* (or *double-lobed Lissajous figure*). This characteristic is used for the faulty localization.

Table 1. DT-PMSM Parameters

Symbol	Parameters	Value and unit
Γ_n	Nominal Torque	$4\ N \cdot m$
N_n	Nominal speed	2000 rpm
p	Pole pairs	4
R_s	Stator resistance	0.435 Ω
L	Inductance in dq axis	0.009 H
L_z	Leakage inductance in $d_z q_z$ axis	0.0015 H
ψ_f	Flux linkage	$0.086\ Wb \cdot T$

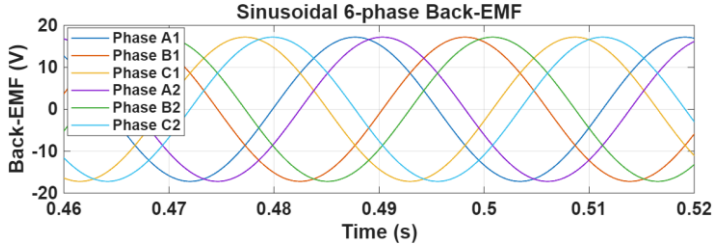

Fig. 4. Sinusoidal 6-phase Back-EMF in the machine with the shifting phase $\pi/6$ at $\omega_m = 477.5$ rpm

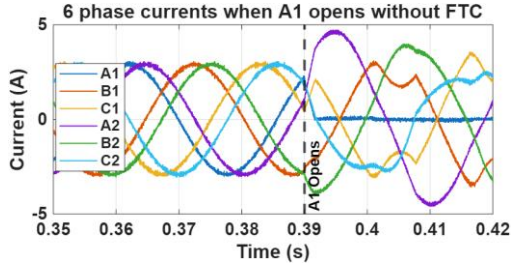

Fig. 5. Six-phase currents when phase A1 opens at 0.39s without FTC

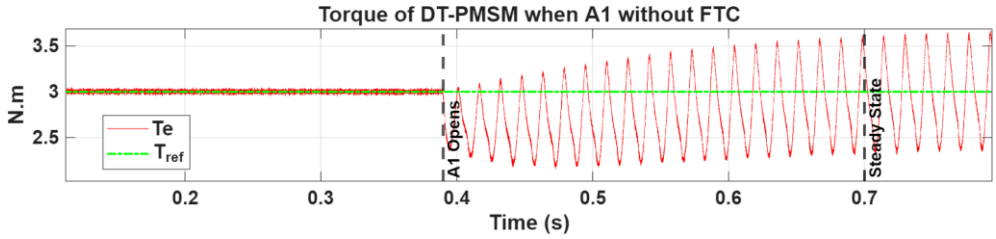

Fig. 6. Electromagnetic Torque without FTC

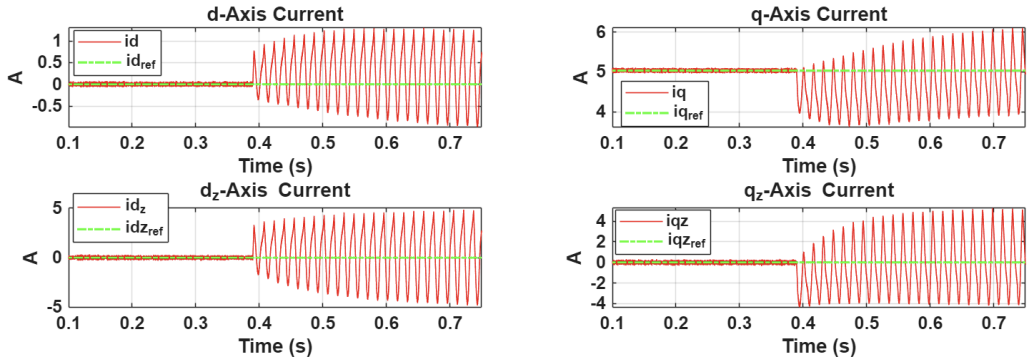

Fig. 7. Rotating frame currents without FTC when A1 opens

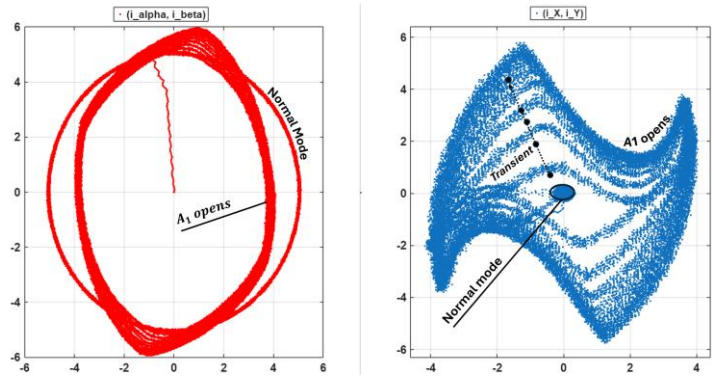

Fig. 8. Trajectories of currents in static frames under both normal and open-phase A1. In normal mode, $\alpha\beta$ subspace forms a circular trajectory while the XY trajectory is a single point at the origin to minimize stator copper losses. When A1 opens, (i_α, i_β) distorts from a perfect circle into a *quasi-elliptical path*, reflecting the loss of symmetry in the fundamental flux. Simultaneously, the (i_X, i_Y) currents expand from the origin to a complex *butterfly-shaped trajectory* (or *double-lobed Lissajous figure*).

To evaluate the proposed PROM-FTC, the simulation scenario is established as shown in Fig.. At 0.3s, phase A1 opens, and then for each period of 0.5s, the other phases (B1 to C2) open sequentially. Only one phase is opened during each interval; the previous faulty phase is restored before the next fault is introduced.

Fig. and Fig. show the value of speed and electromagnetic torque. To prove the robustness of the control method, the speed was investigated in all deceleration, constant, and acceleration periods during faulty intervals while the load torque is always 3 N·m. As the model is *torque control* with a given speed, the demanded electromagnetic torque equals to the load torque. It is observed that despite the occurrence of different open-phase faults, the torque is maintained for well-tracking of reference value. This behavior results from the PROM-FTC which maintain

the (i_d, i_q) through (i_α, i_β) and change (i_{d_z}, i_{q_z}) resonantly via (i_X, i_Y) to compensate for the fault, as illustrated in Fig..

Fig. 13 illustrates the relationship of stationary currents after adding PROM-FTC. Thanks to this method, (i_α, i_β) circular trajectory is successfully maintained unchanged to obtain constant torque, whereas the (i_X, i_Y) are modified by the faults. In particular, (i_X, i_Y) forms a straight line, consistent with the linear dependency derived in previous section. In these trajectories, the symbols from A_1 to C_2 represent for each specific open-phase fault.

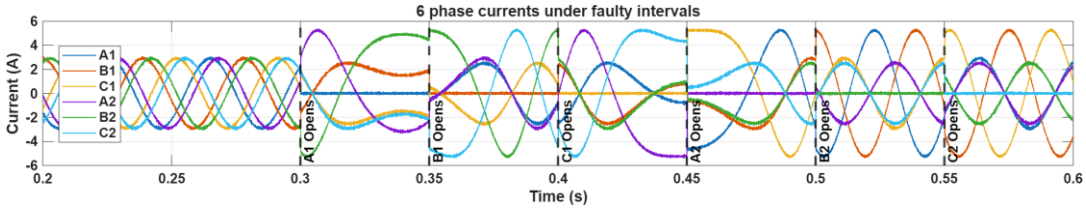

Fig. 9. Six-phase currents under faulty intervals, where one current is opened per period

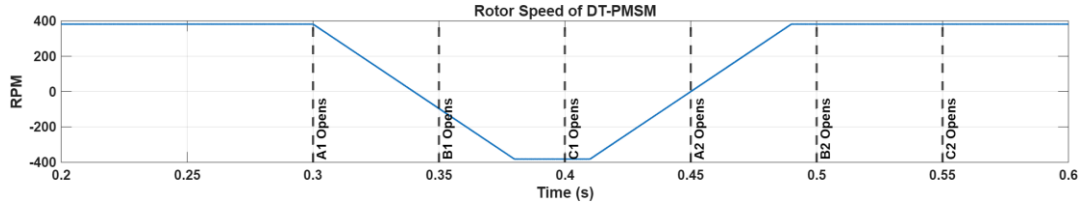

Fig. 10. Rotor speed given in simulation acceleration, constant and deceleration stages

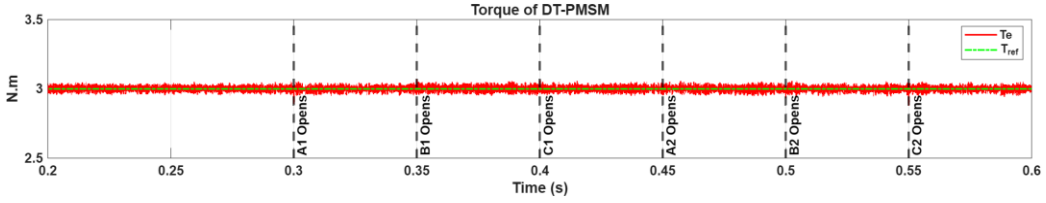

Fig. 11. Electromagnetic torque is maintained constant during faulty periods

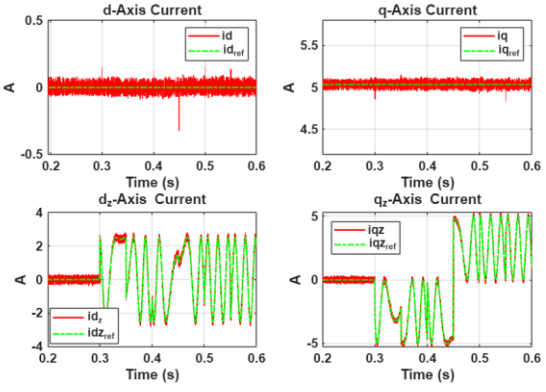

Fig. 12. Rotating frame currents under different faulty conditions, where *dq* currents are constant while $d_z q_z$ currents resonate depending on faulty position

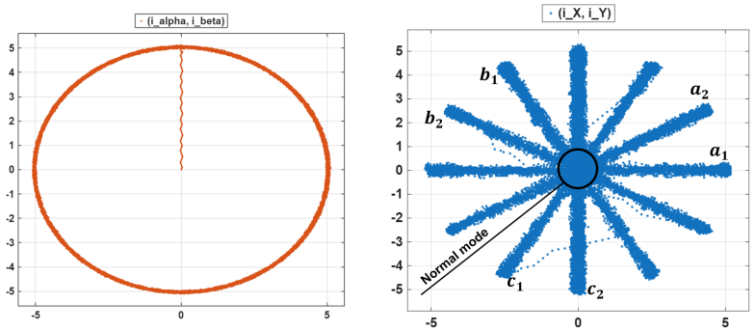

Fig. 13. Trajectories of currents in static frames with PROM-FTC. In faulty mode, $\alpha\beta$ subspace maintains the circular trajectories while XY subspace trajectory changes from a point at origin to lines with different slope depending on faulty position.

5. CONCLUSION

This article proposes a strategy called PROM-FTC, which establishes a general scheme for any single open-phase fault. By analyzing the relationships under faulty conditions and using a permutation matrix within the reduced-order matrix, the method provides a general form of fault-tolerant control. The validity of the proposed model was evaluated in MATLAB/Simulink by introducing a sequence of six single open-phase faults. During the faulty periods, the electromagnetic torque was maintained constantly, demonstrating the efficacy of PROM-FTC. Furthermore, the current trajectories in the stationary frame were analyzed to illustrate their characteristics for each type of fault.

While the specific mathematical matrices developed in this study are tailored to dual three-phase topologies, the underlying methodology for matrix identification provides a generalized framework applicable to other multiphase architectures. The systematic flow which establishes algebraic current constraints based on the specific fault, can be readily adapted to synthesize fault-tolerant control structures for other machines, such as a single 5-phase machine or a triple three-phase machine. It should be noted, however, that applying this methodology to more complex scenarios, such as multiple simultaneous open-phase faults or short-circuit faults, would require the derivation of entirely new reduced-order matrices and modified optimization constraints, as short-circuits introduce active fault current dynamics. Expanding this theoretical framework to accommodate these complex faults, alongside validating the proposed PROM-FTC scheme on a physical hardware prototype, will be the focus of future work. This experimental phase is critical to verify the system's robustness against practical conditions that are not fully captured in simulation, such as inverter dead-time, sensor noise, spatial harmonics, and the real-time execution limits of digital signal processors.

Acknowledgment: This project has been achieved within the framework of EE4.0 (Enerige Electrique 4.0) project. EE4.0 is co-financed by European Union with the financial support of the European Regional Development Fund (ERDF), French State and the French Region of Hauts-de-France.

REFERENCES

[1] L. T. Pham, N. K. Nguyen, and Q. D. Phan, 'Maximum Torque Distribution Per Loss for Dual Three-Phase PMSM for Transportation', in *2025 International Symposium on Electrical and Electronics Engineering (ISEE)*, Oct. 2025, pp. 244–249, doi: https://doi.org/10.1109/ISEE68370.2025.11223479.

[2] M. A. Frikha, J. Croonen, K. Deepak, Y. Benômar, M. El Baghdadi, and O. Hegazy, 'Multiphase Motors and Drive Systems for Electric Vehicle Powertrains: State of the Art Analysis and Future Trends', *Energies*, vol. 16, no. 2, Art. no. 2, Jan. 2023, doi: https://doi.org/10.3390/en16020768.

[3] M. R. Khowja, K. Singh, A. la Rocca, G. Vakil, R. Ramnathan, and C. Gerada, 'Fault-Tolerant Dual Channels Three-Phase PMSM for Aerospace Applications', *IEEE Access*, vol. 12, pp. 126845–126857, 2024, doi: https://doi.org/10.1109/ACCESS.2024.3451705.

[4] W. Zhang, N. K. Nguyen, E. Semail, and Y. Xu, 'A New Harmonic Current Control Approach of Dual Three-Phase PMSM in Degraded Mode', in *IECON 2023- 49th Annual Conference of the IEEE Industrial Electronics Society*, Singapore, Singapore: IEEE, Oct. 2023, pp. 1–6, doi: https://doi.org/10.1109/IECON51785.2023.10312561.

[5] A. G. Yepes, I. Gonzalez-Prieto, O. Lopez, M. J. Duran, and J. Doval-Gandoy, 'A Comprehensive Survey on Fault Tolerance in Multiphase AC Drives, Part 2: Phase and Switch Open-Circuit Faults', *Machines*, vol. 10, no. 3, Art. no. 3, Mar. 2022, doi: https://doi.org/10.3390/machines10030221.

[6] H. Zheng, X. Pei, C. Liagas, C. Brace, and X. Zeng, 'Extended Minimum Copper Loss Range Fault-Tolerant Control for Dual Three-Phase PMSM', *IEEE Trans. Ind. Appl.*, vol. 60, no. 4, pp. 6263–6276, Jul. 2024, doi: https://doi.org/10.1109/TIA.2024.3397637.

[7] L. Xu, H. Ren, T. Jiang, G. Liu, and W. Zhao, 'Minimum Copper Loss Fault-Tolerant Control of Zero Phase Shift Dual Three-Phase SPMSM by Using Reduced-Order Transformation Matrices', *IEEE Trans. Energy Convers.*, pp. 1–10, 2024, doi: https://doi.org/10.1109/TEC.2024.3385010.

[8] Z. Song, Y. Jia, and C. Liu, 'Open-Phase Fault-Tolerant Control Strategy for Dual Three-Phase Permanent Magnet Synchronous Machines Without Controller Reconfiguration and Fault Detection', *IEEE Trans. Power Electron.*, vol. 38, no. 1, pp. 789–802, Jan. 2023, doi: https://doi.org/10.1109/TPEL.2022.3199229.

[9] K. Yu, Z. Wang, M. Gu, and X. Wang, 'Universal Control Scheme of Dual Three-Phase PMSM Drives with Single Open-Phase Fault', *IEEE Trans. Power Electron.*, vol. 37, no. 12, pp. 14034–14039, Dec. 2022, doi: https://doi.org/10.1109/TPEL.2022.3195526.

[10] X. Wang, Z. Wang, M. He, Q. Zhou, X. Liu, and X. Meng, 'Fault-Tolerant Control of Dual Three-Phase PMSM Drives with Minimized Copper Loss', *IEEE Trans. Power Electron.*, vol. 36, no. 11, pp. 12938–12953, Nov. 2021, doi: https://doi.org/10.1109/TPEL.2021.3076509.